

# Fabrication and characterization of electrochemical double layer capacitors using ionic liquid-based gel polymer electrolyte with chemically treated activated charcoal electrodes

Amrita Jain · S. K. Tripathi · Ashish Gupta · Manju Kumari

Received: 9 June 2012 / Revised: 31 August 2012 / Accepted: 7 October 2012 / Published online: 23 October 2012  
© Springer-Verlag Berlin Heidelberg 2012

**Abstract** The present investigation deals with electrochemical double layer capacitors (EDLCs) made up of ionic liquid (IL)-based gel polymer electrolytes with chemically treated activated charcoal electrodes. The gel polymer electrolyte comprising of poly(vinylidene fluoride-co-hexafluoropropylene) (PVdF-HFP)–1-ethyl-2,3-dimethyl-imidazolium-tetrafluoroborate [EDi-MIM][BF<sub>4</sub>]-propylene carbonate (PC)-magnesium perchlorate (Mg(ClO<sub>4</sub>)<sub>2</sub>) exhibits the highest ionic conductivity of  $\sim 8.4 \times 10^{-3} \text{ Scm}^{-1}$  at room temperature ( $\sim 20^\circ \text{C}$ ), showing good mechanical and dimensional stability, suitable for their application in EDLCs. Activation of charcoal was done by impregnation method using potassium hydroxide (KOH) as activating agent. Brunauer–Emmett–Teller (BET) studies reveal that the effective surface area of treated activated charcoal powder ( $1,515 \text{ m}^2 \text{ g}^{-1}$ ) increases by more than double-fold compared to the untreated one ( $721 \text{ m}^2 \text{ g}^{-1}$ ). Performance of EDLCs has been tested using cyclic voltammetry, impedance spectroscopy, and charge–discharge techniques. Analysis shows that chemically treated activated charcoal electrodes have almost triple times more capacitance values as compared to the untreated one.

**Keywords** Ionic liquid · Gel polymer electrolytes · Electrochemical double layer capacitors · Impedance spectroscopy · Charge–discharge

## Introduction

Supercapacitors, known as important charge storage devices, offer an interesting and technologically relevant compromise with respect to energy density and power density [1–4]. Supercapacitors are attracting recent attention due to the increasing demand of a new kind of electric power sources having high specific power and long stability/cycle life for their use in electrochemical vehicles and many other applications [5–7]. Basically, there exist two types of supercapacitors which are differentiated on the basis of energy storage mechanisms: electrochemical double layer capacitors (EDLCs) and redox supercapacitors [8]. In EDLCs, charge storage mechanism is electrostatic in nature and different types of carbonaceous materials and their derivatives like activated carbon powder/fiber/fabrics [9–12], activated carbon composites like AC/PbO<sub>2</sub>, AC/NiO<sub>2</sub> [13, 14], etc. are used as electrode materials. On the other hand, electroactive oxides like manganese oxide (MnO<sub>2</sub>) [15–19], iron oxide [20], vanadium oxide (V<sub>2</sub>O<sub>5</sub>) [21], and nickel oxide [22] or conducting polymers like polypyrrole [23–26], polyaniline [27–29], polythiophene [8, 24, 30], etc. are used as active electrodes in redox supercapacitors. In redox supercapacitors, faradic redox reactions at electrode/electrolyte interfaces take place which leads to pseudocapacitance. For the fabrication of EDLCs, liquid electrolytes including aqueous and organic solutions are extensively chosen and are reported in literature [31]. However, devices with liquid electrolytes have the risk of liquid leakage, pollution to the environment, bulky design, corrosion, and loss of electrolyte through drying. As a result, gel polymer electrolyte is greatly needed to replace the liquid one because of its high ionic conductivity, wide operation temperature, electrochemical window, and almost no leakage [32]. A few recent reports include the EDLCs based on different polymer/gel electrolyte, for e.g., PMMA–ethylene carbonate (EC)-propylene

A. Jain · S. K. Tripathi (✉) · A. Gupta  
Department of Physics,  
Jaypee University of Engineering and Technology,  
AB Road,  
Raghogarh 473226, Guna, India  
e-mail: sktripathi16@yahoo.com

M. Kumari  
Department of Chemistry, Viva Institute of Technology,  
Thane, Maharashtra, India

carbonate (PC)–NaClO<sub>4</sub> [33], PVA–H<sub>3</sub>PO<sub>4</sub> [34], PEO–PEG–LiCF<sub>3</sub>SO<sub>3</sub> [35], etc. Mostly, lithium salts were used to synthesize polymeric electrolytes in order to achieve good ionic conductivity and mechanical stabilities for their application in electrochemical device fabrication, particularly lithium-ion-based batteries [36]. Nowadays, in substitution to lithium salts, magnesium ion-based gel electrolytes were showed more attention due to its comparable results in terms of its ionic conductivities, mechanical stabilities, environment friendliness, and nonexplosive natures. Magnesium ion-based polymer gel electrolyte has not been widely reported, except for few systems with aprotic organic plasticizers such as EC, PC and diethyl carbonate (DEC) [37, 38].

In recent years, room temperature ionic liquids (RTILs) have been proposed as nonvolatile polar media in a variety of electrochemical systems [39, 40]. They are room-temperature molten salts that typically consist of bulky asymmetric organic cations and inorganic anions. They have many interesting properties like nonvolatility, nonflammability, excellent thermal stability, high ionic conductivity, and wider electrochemical potential window, which make them suitable for application as electrolyte in energy storage devices like batteries and supercapacitor [39–44].

Activated charcoal is quite cheap and an easily available material on the commercial scale, which is mostly used for medical purposes, particularly, as an adsorbent of particles and gases in the digestive system. It is also used as an electrode material for device fabrication in different types of energy storage devices, particularly, supercapacitors, because of its high electrical conductivity and large specific surface area with almost the same charge storage capability as compared with the reported devices based on the other carbonaceous electrode materials.

In the present study, suitability of ionic liquid (IL)-based gel polymer electrolytes comprising of poly(vinylidene fluoride-co-hexafluoropropylene) (PVdF-HFP)–1-ethyl-2,3-dimethyl-imidazolium-tetrafluoroborate [EDiMIM][BF<sub>4</sub>]–PC–magnesium perchlorate (Mg(ClO<sub>4</sub>)<sub>2</sub>) has been tested successfully with chemically treated activated charcoal powder-based electrodes for the fabrication of EDLCs. The performance characteristics of the EDLCs in the present study have been carried out using a.c. impedance spectroscopy, linear sweep cyclic voltammetry, galvanostatic charge–discharge test and prolonged cyclic tests.

## Experimental details

### Electrolyte preparation

[EDiMIM][BF<sub>4</sub>], (PVdF-HFP) as polymer and Mg(ClO<sub>4</sub>)<sub>2</sub> as salt were purchased from Sigma-Aldrich and used as received. Solution cast technique was used to prepare the

film of polymer gel electrolyte. In the process, initially, the liquid electrolyte was optimized and prepared by dissolving 0.3 M magnesium salt (Mg salt) in PC. The polymer PVdF-HFP and IL [EDiMIM][BF<sub>4</sub>] were separately dissolved in acetonitrile. The liquid electrolyte was then mixed with the solution of PVdF-HFP/[EDiMIM][BF<sub>4</sub>]/acetonitrile in different weight ratios and stirred magnetically for 4–5 h. The concentration of PVdF-HFP and [EDiMIM][BF<sub>4</sub>] was optimized and controlled at a ratio of 7:3. The viscous mixture was cast over glass petri dishes and acetonitrile was allowed to evaporate slowly, thereafter, free standing polymer gel electrolyte films (thickness ~400–450 μm) were obtained. Finally, the optimized polymer gel electrolyte of the following composition: {PVdF-HFP (70 wt.%)–[EDiMIM][BF<sub>4</sub>] (30 wt.%)}(20 wt.%)–{PC–Mg(ClO<sub>4</sub>)<sub>2</sub> (0.3 M)}(80 wt.%) was used for the fabrication of supercapacitor cell.

### Synthesis of chemically treated activated charcoal powder

Activated charcoal (Loba Chemie) was used as a precursor in the present study. Five grams of activated charcoal was mixed by stirring a solution containing 15 ml of double distilled water with activating agent KOH for 2 h at 60 °C in 1:1 ratio. The resulting slurry was dried at 110 °C for 12–14 h in an oven. Then, the resulting mixture was used for activation, carried out in a muffle furnace, and the sample was heated (10 °C min<sup>-1</sup>) from room temperature to the final carbonization temperature ( $T_{\text{carb}}=600$  °C) in the presence of nitrogen flow (150 mlmin<sup>-1</sup>). The sample was kept at the final temperature for 1 h before cooling down to room temperature under same nitrogen flow. The pyrolyzed sample was washed repeatedly with 5 M HCl solution and later with double distilled water until it is free from chloride ions. After removal of activating agent, the sample was dried at 110 °C for 12–14 h.

### Preparation of electrodes

The electrodes were prepared by making slurry of chemically treated activated charcoal powder and PVdF-HFP in the ratio 90:10 (w/w) in a common solvent acetone by thorough mixing. Fine films of electrodes were coated by spraying the slurry on carbon cloth (Ballard, USA) and kept in oven at 70 °C for 10–12 h. The same procedure was followed for making untreated activated charcoal powder-based electrodes on the same carbon clothes.

### Characterization of electrodes

The morphology of the chemically treated and untreated activated charcoal powder electrodes was examined using scanning electron microscopy (SEM) with the help of JSM-6360, JEOL/EO. Nitrogen adsorption–desorption isotherms

were measured at 77 K using Micromeritics Instruments, Gemini Model 2380 analyzer after heating the sample at 100 °C for 2 h. The Brunauer–Emmett–Teller (BET) surface area of the samples was measured using nitrogen adsorption data over a relative pressure ranging from 0.05 to 1.0.

#### Electrochemical measurements

The electrical conductivity of gel polymer electrolyte films was evaluated by means of an AC impedance technique using a computer-controlled LCR HiTester (Hioki 3522–50, Japan model) over the frequency range of 100 kHz to 1 Hz with a signal level of 10 mV. The EDLCs were fabricated using chemically treated and untreated activated charcoal powder-based electrodes with optimized composition of polymer gel electrolyte which was sandwiched between two symmetrical electrodes.

In AC impedance measurements, the overall capacitance  $C$  of the capacitor cells was evaluated by using the relation:

$$C = -1/\omega Z'' \quad (1)$$

where  $\omega$  is the angular frequency and  $Z''$  is the imaginary part of the total complex impedance. The single-electrode specific capacitance of the capacitor cells was evaluated by multiplying the overall capacitance by a factor of two and dividing the result by the mass of the single-electrode material.

The linear sweep cyclic voltammetry was carried out by using a computer-controlled CHI 608C (CH Instruments, USA). The capacitance values from this technique were evaluated by using the relation:

$$C = i/s \quad (2)$$

where  $i$  is the measure of constant current and  $s$  is the scan rate.

The charge–discharge characteristics of the capacitor cells were performed at constant current and its discharge capacitance  $C_d$  was calculated from the linear part of the discharge curves using the relation:

$$C_d = i\Delta t/\Delta V \quad (3)$$

where  $i$  is the constant current and  $\Delta t$  is the time interval for the voltage change  $\Delta V$ .

The Coulombic efficiency,  $\eta$ , was calculated using the following equation, when the same current is used for charging and discharging:

$$\eta = (t_D/t_C) \times 100\% \quad (4)$$

where  $t_D$  and  $t_C$  are the galvanostatic discharging and charging times, respectively.

## Results and discussions

### Characteristics of gel electrolytes

The composition of {PVdF-HFP (70 wt.%)–[EDIMIM][BF<sub>4</sub>] (30 wt.%)}(20 wt.%)–{PC–Mg(ClO<sub>4</sub>)<sub>2</sub> (0.3 M)}(80 wt.%)–based polymer gel electrolyte was optimized to get highly conducting, mechanically stable, and flexible films for their application as electrolyte materials in EDLCs. Synthesis and optimization of gel polymer electrolytes has been carried out in three different stages, which broadly includes synthesis and optimization of liquid electrolytes, polymer blend, and finally, gel polymer electrolytes. For this purpose, first of all, liquid electrolyte comprising of PC–Mg(ClO<sub>4</sub>)<sub>2</sub> was synthesized and optimized by the addition of Mg salt in PC. Figure 1 shows the variation of ionic conductivity of liquid electrolyte PC–Mg(ClO<sub>4</sub>)<sub>2</sub> as a function of salt concentration. Initially, the conductivity of pure solvent, PC was measured at room temperature (~25 °C) and found to be  $8.3 \times 10^{-6} \text{ S cm}^{-1}$ . A gradual increase in conductivity is observed, when Mg salt is added in PC up to 0.3 M and thereafter, conductivity remains almost constant up to 0.8 M. Further addition of salt beyond the concentration of 0.8 M leads to the decrease in conductivity of liquid electrolytes. It can be explained in the following manner. Initially, as the salt concentration increases, the number of free mobile ions also increases, which leads to the increase in conductivity. At higher concentrations of the salt, ion aggregation is likely to play a major role in limiting the ionic conductivity of the electrolyte [45]. Hence, in this way, we have chosen the optimized composition of liquid electrolyte as PC–Mg(ClO<sub>4</sub>)<sub>2</sub> (0.3 M) for the synthesis of polymeric gel electrolytes.

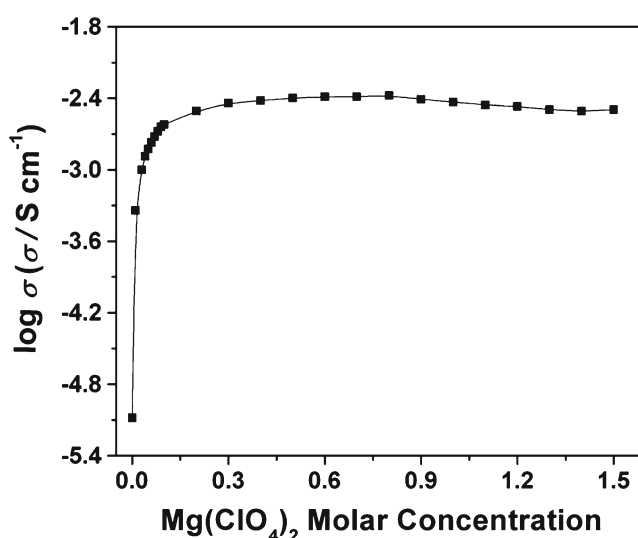


**Fig. 1** Variation of ionic conductivity of liquid electrolyte as a function of salt concentration

In the second stage, a blend of polymer PVdF-HFP and IL [EDiMIM][BF<sub>4</sub>] was synthesized and optimized separately in common solvent acetonitrile. Figure 2 shows the variation of ionic conductivity of (polymer + IL) (PVdF-HFP + [EDiMIM][BF<sub>4</sub>]) blend as a function of IL concentration measured in different weight percents with respect to the host polymer, PVdF-HFP. In this process, first of all, conductivity of the host polymer, PVdF-HFP, was measured and it was found to be  $\sim 10^{-10} \text{ S cm}^{-1}$ . A gradual increase in conductivity is observed by the addition of IL [EDiMIM][BF<sub>4</sub>] up to 30 wt.%, which is measured as  $4 \times 10^{-5} \text{ S cm}^{-1}$ . On further addition of IL in the host polymer beyond 30 wt.%, conductivity of the polymer blend system decreases and thereafter, it remains constant, as can be depicted from Fig. 2. The possible reason of enhancement in conductivity is due to the combined effect of plasticization, which leads to the enhanced flexibility in the polymer backbone and the generation/introduction of mobile-charged species, namely, [EDiMIM]<sup>+</sup> and [BF<sub>4</sub>]<sup>-</sup>, in the polymer IL blend system. The decrease in conductivity observed after  $\sim 30$  wt.% of IL, [EDiMIM][BF<sub>4</sub>], is due to the ion association effect of the component ions of the IL [EDiMIM][BF<sub>4</sub>]. In this way, we have chosen the optimized blend as PVdF-HFP (70 wt.%) + [EDiMIM][BF<sub>4</sub>] (30 wt.%) for further synthesis of polymer gel electrolyte by maintaining the polymer to IL weight ratio of 7:3.

Finally, the polymer gel electrolyte comprising of PVdF (HFP)–[EDiMIM][BF<sub>4</sub>]–PC–Mg(ClO<sub>4</sub>)<sub>2</sub> was synthesized and optimized by immobilizing different weight percents of the optimum concentration of polymer IL blend {PVdF-HFP (70 wt.%) + [EDiMIM][BF<sub>4</sub>] (30 wt.%)} in the solution of optimized liquid electrolyte PC–Mg(ClO<sub>4</sub>)<sub>2</sub> (0.3 M) system as shown in Fig. 3. It can be clearly depicted from the figure that the initial conductivity of liquid electrolyte

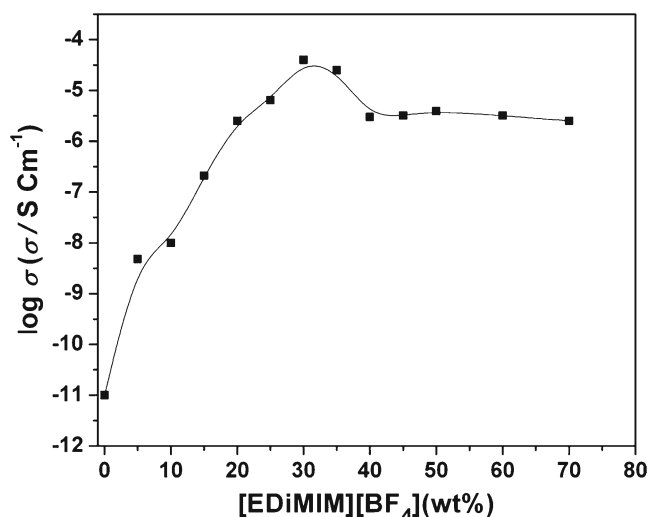


**Fig. 2** Room temperature ionic conductivity of polymer ionic liquid blend as a function of ionic liquid concentration

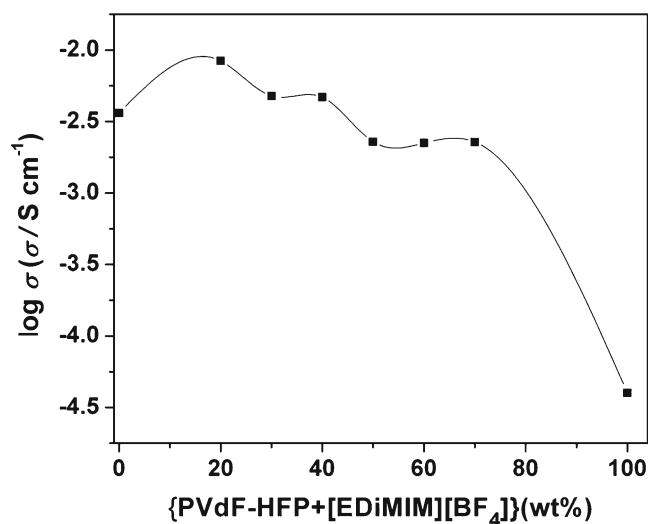


**Fig. 3** Variation of ionic conductivity of polymer gel electrolyte as a function of polymer ionic liquid blend concentration

without blend is  $3.63 \times 10^{-3} \text{ S cm}^{-1}$ . On the addition of optimum blend {PVdF-HFP(70 wt.%) + [EDiMIM][BF<sub>4</sub>](30 wt.%)} in the optimized liquid electrolyte PC–Mg(ClO<sub>4</sub>)<sub>2</sub> (0.3 M) solution, the ionic conductivity of gel polymer electrolyte initially increases (slightly) and shows a maxima ( $\sim 8.4 \times 10^{-3} \text{ S cm}^{-1}$ ) at 20 wt.% of blend and then it decreases on its further addition. It has been observed that when the concentration of blend varies between 0 and 20 wt.%, the film of the polymer gel electrolyte is found to be mechanically unstable. The stable film is obtained only after 20 wt.% of the blend concentration. Such type of increase in conductivity behavior of the polymer gel electrolyte on addition of polymer concentration has been reported earlier by some workers [46, 47] in a different polymeric system. The distinct initial increase in the conductivity due to the addition of a host polymer blend in the liquid electrolyte may be explained by the ‘breathing chain model’ as proposed by Chandra et al. [47, 48]. According to this model, polymeric gels are considered to consist of dissociated ions (free ions), ion pairs, undissociated salts, solvents, and polymeric chains existing either in folded or partially/fully unfolded form. At lower concentration of the blend, the system behaves like liquid electrolytes as a result of dissociation of salts. With an increase in blend contents beyond 20 wt.%, the viscosity of the electrolyte solutions increases and it tends to decrease the mobility of free ions which further leads to the decrease in the conductivity of the gel electrolytes. In a lower concentration region below 20 wt.% of the blend content, it is assumed that at a microscopic level, the polymer chain ‘breathes’ when it opens or folds by occupying different volumes at different time spans. Hence, folding and unfolding of the polymeric chain leads to the localized pressure fluctuations in the surrounding volumes and this localized turbulent pressure leads to

the further dissociation of ion pairs and hence, enhances the mobility and conductivity of the system. Due to this reason, the higher conductivity of polymer gel electrolyte as compared to pure liquid electrolyte is observed at lower concentration of the polymer IL blend. In this way, the final composition of polymer gel electrolyte {PVdF-HFP (70 wt.%)–[EDiMIM][BF<sub>4</sub>] (30 wt.%)}{20 wt.}%–{PC–Mg(ClO<sub>4</sub>)<sub>2</sub> (0.3 M)}{80 wt.}% has been chosen as electrolyte materials for the fabrication of EDLCs.

#### SEM studies

SEM was used to investigate the surface morphology of the treated and untreated activated carbon-based electrode. Figure 4a shows the surface morphology of chemically treated activated carbon. The external surface is full of cavities and has large surface area. According to the micrograph, it seems that the cavities resulted from the removal of potassium hydroxide during preparation, leaving the space that was previously occupied by the activating agent,

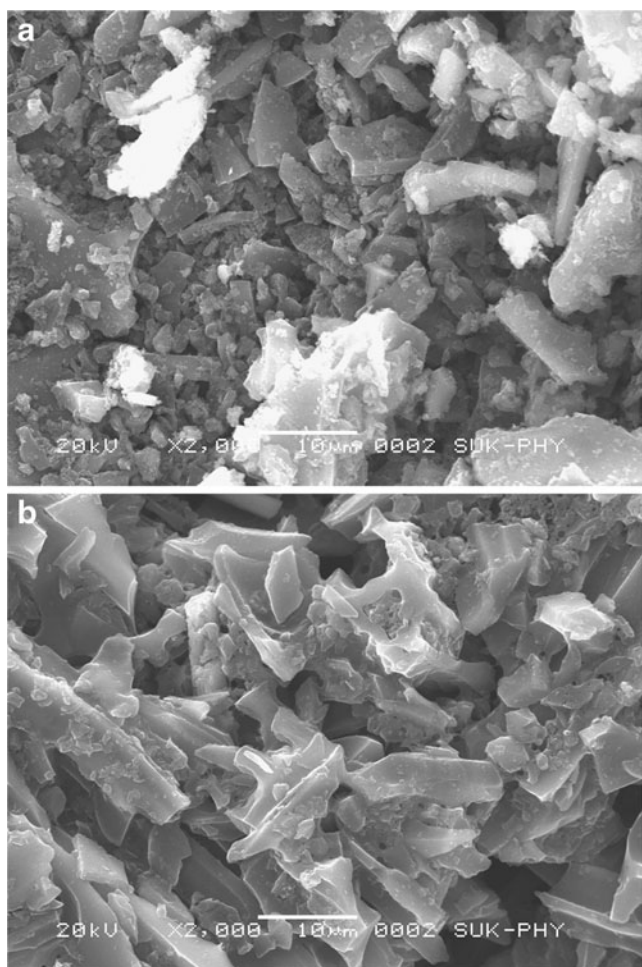


**Fig. 4** SEM image of **a** chemically treated activated charcoal electrode and **b** untreated activated charcoal electrode

thereby providing larger surface area which is believed to be desirable for the application of supercapacitor; hence, it shows eximious electrochemical performances. The carbonization temperature for chemical activation was quite low to cause the agglomeration of the char structure. It is clear from the SEM image that chemically treated activated charcoal resembles honeycombed surface which helps in providing rapid access of the electrolyte into the bulk phase of the electrode material, thereby increasing the utilization ratio of the active substance; hence, the specific capacitance of the electrode material is aggrandized. Figure 4b shows the SEM micrograph of untreated activated charcoal that lacks porosity; texture has less active site for electrostatic charge accumulation which does not facilitate the charge transfer with the electrode materials.

#### Porous texture characterization

The adsorption isotherm shown in Fig. 5 was employed to calculate the BET surface area and porous volumes and the results are summarized in Table 1. Both samples have type I isotherms, which is characteristic of microporous solids. As expected from N<sub>2</sub> adsorption data at 77 K, the surface area and pore volume have remarkably increased upon activation. The surface area for chemically treated activated charcoal is 1,515 m<sup>2</sup>g<sup>-1</sup>, whereas it is 721 m<sup>2</sup>g<sup>-1</sup> for untreated charcoal powder. It is clear from the values that chemically activated charcoal powder has almost double BET surface area as compared to untreated charcoal powder. The treated activated charcoal powder has relatively broader knee which indicates the presence of pores of larger size. The volume of micropores is also higher for treated activated charcoal powder which suggests that activating agent

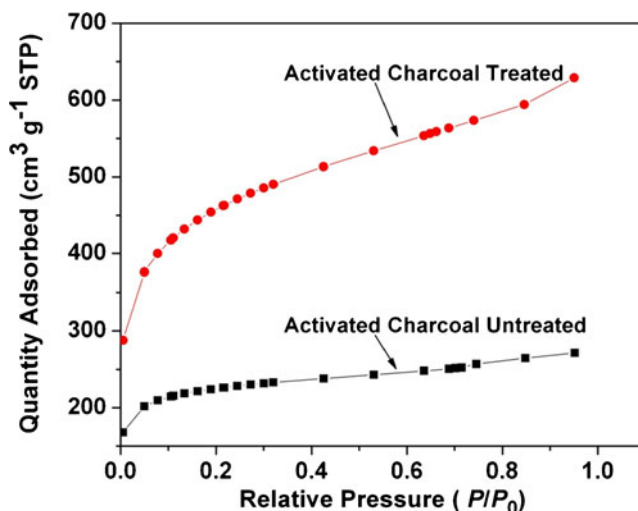


**Fig. 5** N<sub>2</sub> adsorption isotherms of chemically treated activated charcoal powder and untreated charcoal powder at 77 K

**Table 1** BET surface areas and micropore volume of treated and untreated activated charcoal powder

Sample	BET surface area (m <sup>2</sup> g <sup>-1</sup> )	Micropore volume (cm <sup>3</sup> g <sup>-1</sup> )
AC (T)	1,515	0.329924
AC	721	0.252381

AC (T) Treated activated charcoal, AC untreated activated charcoal

promotes the development of new micropores and widening of the already developed ones. The isotherm of

Cell A : AC(T) | {PVdF – HFP(70 wt.%) – [EDiMIM][BF<sub>4</sub>](30 wt.%) } {20 wt.%} – {PC – Mg(ClO<sub>4</sub>)<sub>2</sub>(0.3 M)} {80 wt.%} | AC(T)  
 Cell B : AC | {PVdF – HFP(70 wt.%) – [EDiMIM][BF<sub>4</sub>](30 wt.%) } {20 wt.%} – {PC – Mg(ClO<sub>4</sub>)<sub>2</sub>(0.3 M)} {80 wt.%} | AC

where AC (T) is chemically treated activated charcoal powder electrode on carbon cloth, and AC is untreated activated charcoal powder electrode on same carbon cloth.

In order to characterize EDLCs, different physical techniques like ac impedance spectroscopy, linear sweep cyclic voltammetry (with prolonged cyclic tests), galvanostatic charge–discharge tests have been adopted.

#### Impedance spectroscopy

Figure 6a–b shows the complex impedance plot of EDLC cells (A–B). The impedance spectroscopy is a well-known technique for electrochemical characterization of supercapacitors, which enables the evaluation of various parameters that are associated with bulk properties of electrolytes and electrode interfaces including equivalent series resistance (ESR) of the capacitors, potential dependent faradic resistances, low frequency capacitance values, etc. to be evaluated in different frequency ranges [5]. It should be noted that the impedance behavior of an ideal capacitor is a straight line parallel to the imaginary axis of the complex impedance plots. However, in real capacitors, the steep rising capacitive impedance response is observed in the lower frequency region along with the high frequency semicircular features owing to the bulk and interfacial properties of the capacitor cells. In the present studies, an almost ideal behavior of impedance plot is observed for chemically treated activated charcoal powder-based electrodes, i.e., steep rising behavior in the lower frequency region as can be seen from Fig. 6a–b and semicircular spurs have also been distinctly observed in higher frequency region (inset of Fig. 6a) and

the chemically treated activated charcoal powder shows: (1) a sharp adsorption at very low relative pressures that is a typical feature of materials having micropores and (2) a hysteresis at medium to high relative pressure indicating the presence of mesopores.

#### Characteristics of EDLCs

Different EDLC cells of the following configuration have been constructed using chemically treated and untreated activated charcoal powder electrodes with optimized polymeric gel electrolyte:

depressed spur is observed in case of untreated activated charcoal powder-based electrodes. This response is associated mainly with the interfacial characteristics having a specific porous structure of the electrode material in contact with the highly flexible and mechanically stable polymeric gel electrolyte. The impedance response of various possible geometries for the porous structure of the electrode material has been described theoretically by some workers [5, 49]. Keiser et al. [49] derived relations for the impedance as a function of frequency for various geometries of a single pore and applied the results to the case of porous electrodes. A comparison of the impedance response observed in the present case with the theoretical studies mentioned above [49] reveals that the chemically treated activated charcoal powder electrodes possess almost cylindrical geometry of the pores accessible to the gel electrolytes. Such overall response of the EDLCs indicates that the equivalent circuit should be represented by a modified Randles circuit as can be seen from the Fig. 6c. The semicircle which is slightly suppressed towards the real axis is attributed to the parallel combination of double layer capacitance,  $C_{dl}$ , and charge transfer resistance,  $R_{ct}$ , in series with Warburg impedance. The Warburg impedance is related with diffusional process of ions at the porous electrode–electrolyte interface, which corresponds to the transmission line type RC equivalent circuit [5]. Various electrical parameters such as bulk resistance,  $R_b$ , charge transfer resistance,  $R_{ct}$ , total resistance,  $R$ , and capacitance  $C$  (as calculated using Eq. 1) at frequencies 10 mHz and 1 mHz is summarized in Table 2. An attractive aspect of the present study is that there is a tremendous improvement in the values of capacitance and almost

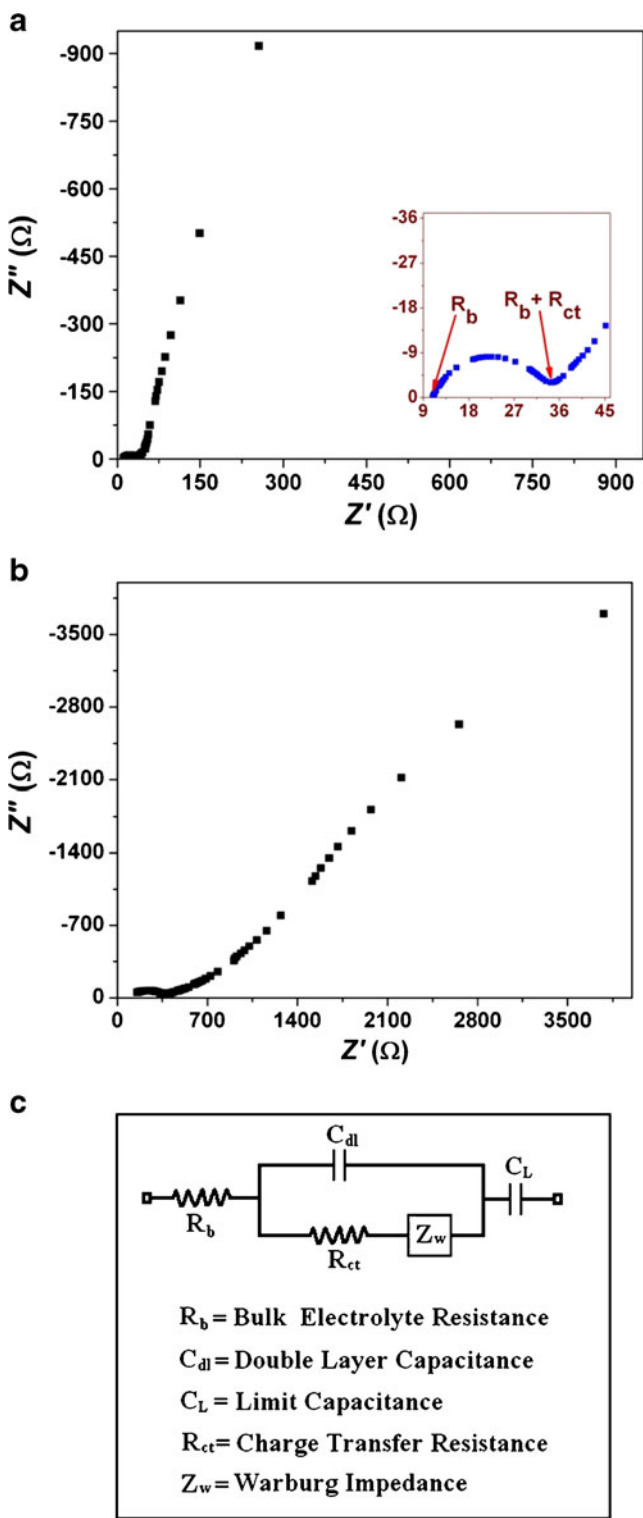


**Fig. 6** Typical impedance plot of different EDLC cells. **a** Cell A: AC (T) | PVdF-HFP-[EDiMIM][BF<sub>4</sub>]-PC-MgClO<sub>4</sub>)<sub>2</sub> | AC(T). **b** Cell B: AC | PVdF-HFP-[EDiMIM][BF<sub>4</sub>]-PC-MgClO<sub>4</sub>)<sub>2</sub> | AC. **c** Modified Randles circuit, representing an equivalent circuit for the capacitor cells

negligible values of  $R_b$ ,  $R_{ct}$ , and  $R$  is observed for treated activated charcoal powder-based electrodes as compared to the untreated one. In the forthcoming section, utility of supercapacitors is also validated by analyzing its impedance data by using complex capacitance and complex power method.

Complex capacitance and complex power analysis

Bode plots, the real  $C'(\omega)$  and imaginary part  $C''(\omega)$  of the complex capacitance  $C(\omega)$  as a function of frequency, are useful for gaining insight into the electrochemical properties of EDLCs [50]. Bode plots for  $C'(\omega)$  for cell A–B are shown in Fig. 7a–b. The dielectric relaxation time or relaxation time constant,  $\tau_0$  of the supercapacitor [51] corresponds to the figure of merit of the electrochemical devices [52]. This is also one of the most important parameters which shows discharge characteristics and has been calculated by other workers for various cell assemblies based on complex capacitance and complex power analysis by using impedance data [53, 54].

The overall complex capacitance is calculated by using the relation:

$$C(\omega) = C'(\omega) - jC''(\omega). \tag{4}$$

$C'(\omega)$  and  $C''(\omega)$  are calculated by using the relations:

$$C'(\omega) = -Z''(\omega) / \{ \omega |Z(\omega)|^2 \} \tag{5}$$

$$C''(\omega) = Z'(\omega) / \{ \omega |Z(\omega)|^2 \} \tag{6}$$

where  $Z'(\omega)$  and  $Z''(\omega)$  are, respectively, real and imaginary parts of the complex impedance,  $Z(\omega)$  and  $\omega$  is the angular frequency which is given by  $\omega = 2\pi f$ .

At low frequency,  $C'(\omega)$  corresponds to the capacitance of the electrode material and  $C''(\omega)$  represents the energy dissipation by an irreversible process that represents the hysteresis of the materials [54]. From Fig. 7a–b, it can be seen that at lower frequency of 1 mHz, the values of capacitance is found to be 812 mF cm<sup>-2</sup> for treated activated charcoal-based EDLCs, which is appreciably higher than that of the untreated one having capacitance of the order of 106 mF cm<sup>-2</sup>. With the increase of frequency, the capacitance exhibits a frequency dependency behavior, and  $C'(\omega)$  drops sharply in the region of 5–50 mHz. At higher frequency, the capacitance is insignificant and the EDLCs behave like a pure resistance. The  $C''(\omega)$  with frequency is given in

**Table 2** Electrical parameters of different EDLC cells from impedance analysis

Cells	$R_{ct}$ ( $\Omega\text{cm}^2$ )	$R_b$ ( $\Omega\text{cm}^2$ )	10 mHz		1 mHz			
			$R$ ( $\Omega\text{cm}^2$ )	$C$ ( $\text{mF cm}^{-2}$ ) <sup>a</sup>	$R$ ( $\Omega\text{cm}^2$ )	$C$ ( $\text{mF cm}^{-2}$ ) <sup>a</sup>		
							$C$ ( $\text{F g}^{-1}$ ) <sup>b</sup>	
A	4.6	2.3	13.8	618.3	412.2	51.2	868.4	578.9
B	48.4	30.5	303.2	70.6	20.2	755.8	215.1	61.5

<sup>a</sup>Overall capacitance of the cells<sup>b</sup>Single-electrode specific capacitance of the cells

Fig. 8a–b. As per the convention, the maximum point of the curve represents the complete system, which describes the transition point at which the circuit changes its behavior from purely resistive to purely capacitive character [50].

Complex power of the fabricated cell was calculated by using the relation:

$$S(\omega) = P(\omega) + jQ(\omega) \quad (7)$$

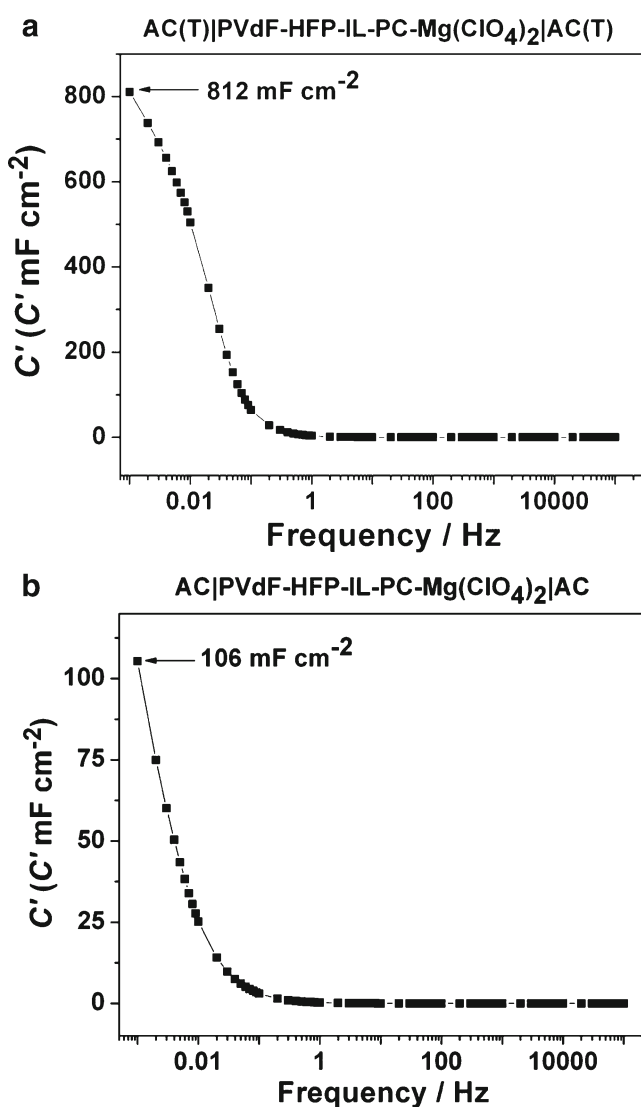


**Fig. 7** Typical plots for the real part of complex capacitance [ $C'(\omega)$ ] as a function of frequency (in logarithmic scale) for different EDLC cells. **a** Cell A: AC(T) | PVdF-HFP-[EDiMIM][BF<sub>4</sub>]-PC-MgClO<sub>4</sub>)<sub>2</sub> | AC(T). **b** Cell B: AC | PVdF-HFP-[EDiMIM][BF<sub>4</sub>]-PC-MgClO<sub>4</sub>)<sub>2</sub> | AC

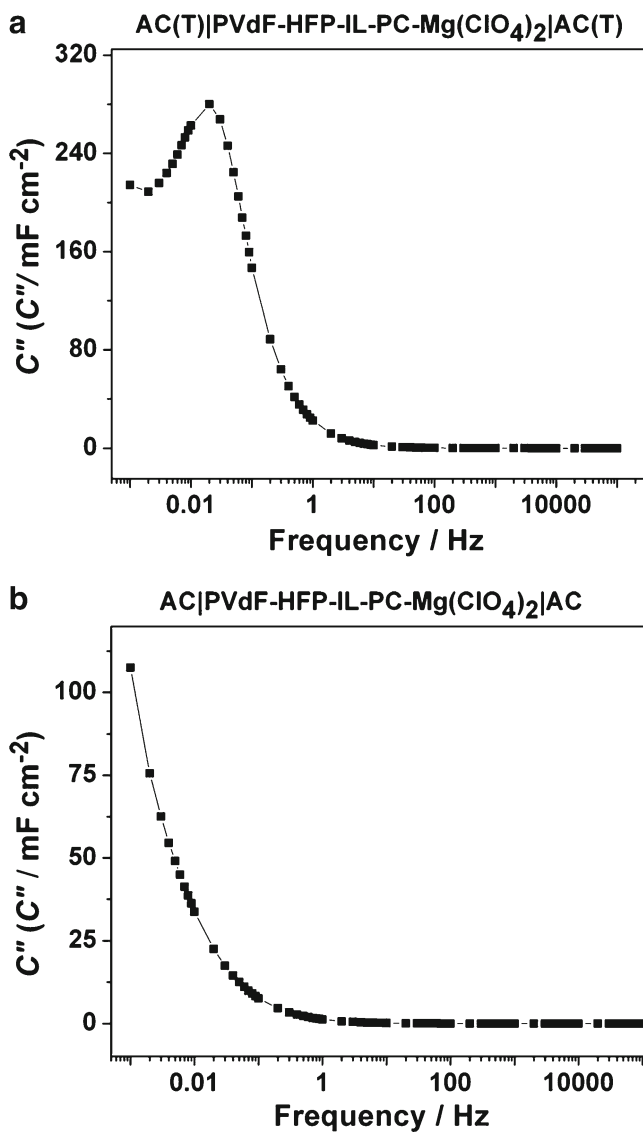


**Fig. 8** Typical plots for the imaginary part of complex capacitance [ $C''(\omega)$ ] as a function of frequency (in logarithmic scale) for different EDLC cells. **a** Cell A: AC(T) | PVdF-HFP-[EDiMIM][BF<sub>4</sub>]-PC-MgClO<sub>4</sub>)<sub>2</sub> | AC(T). **b** Cell B: AC | PVdF-HFP-[EDiMIM][BF<sub>4</sub>]-PC-MgClO<sub>4</sub>)<sub>2</sub> | AC



where  $P(\omega)$  is the real part of complex power which is also known as active power and  $Q(\omega)$  is the imaginary part of complex power and it is also known as reactive power.  $P(\omega)$  and  $Q(\omega)$  are evaluated by using the relation:

$$P(\omega) = \omega C''(\omega) |\Delta V_{rms}|^2 \tag{8}$$

$$Q(\omega) = -\omega C'(\omega) |\Delta V_{rms}|^2 \tag{9}$$

where  $|\Delta V_{rms}|^2 = \Delta V_{max} / \sqrt{2}$  with  $V_{max}$  being the maximum amplitude of the AC signal.

The insight of relaxation time constant,  $\tau_0$ , is basically a quantitative measure of how fast the device can be charged and discharged reversibly. The relaxation time constant,  $\tau_0 = 1/2\pi f_0$  can be calculated from the plots of  $C'(\omega)$  vs. frequency and  $C''(\omega)$  vs. frequency. From the frequency corresponding to half of the maximum value of  $C'(\omega)$ , the relaxation time constant ( $\tau_0$ ) can be evaluated. The change of  $C''(\omega)$  with frequency attains a maximum value at frequency,  $f_0$ , from which the value of  $\tau_0$  can be calculated. Figure 8a and b shows the variation of  $C''(\omega)$  with frequency for cells A–B. The plot shows a characteristic hysteresis for both cells A and B which is under investigation. It can be noted that chemically treated activated charcoal-based EDLC shows a clear peak formation, whereas EDLC based on untreated activated charcoal electrode have not even reached the maxima even at the lowest frequency of 1 mHz, used in the present investigation.

The plots of  $|P|/|S|$  and  $|Q|/|S|$  of the complex power vs. frequency (expressed in logarithmic scale) for cells A–B are shown in Fig. 9a–b. From these plots, we can find out the relaxation time constants for both cells (A–B). The power dissipated into the system can be analyzed from the normalized active power which is denoted by  $|P|/|S|$ . At high frequency, when supercapacitor behaves like a pure resistor, all the power is dissipated into the system ( $P=100\%$ ); on the other hand, at low frequency, no power is dissipated into a pure capacitance. The intersection of two plots occurs at frequency  $f_0$ , which is also known as resonance frequency with the help of which relaxation time constant  $\tau_0 (=2\pi f_0)$  can be determined explicitly. This time constant,  $\tau_0$ , belongs to the phase angle of  $45^\circ$  and it represents the behavioral change of supercapacitor from purely resistive to purely capacitive. It will act as pure resistor for the frequency  $f > 1/\tau_0$  and pure capacitor for the frequency  $f < 1/\tau_0$ .

From the crossing of two plots at a frequency  $f_0$ , the value of  $\tau_0$  has been calculated. The calculated relaxation time constant  $\tau_0$  for cells A and B are 5.3 s and 8.0 s, respectively. This clearly indicates that the chemically treated activated charcoal-based EDLCs provide the faster delivery of stored energy as compared to the untreated one at the higher power.

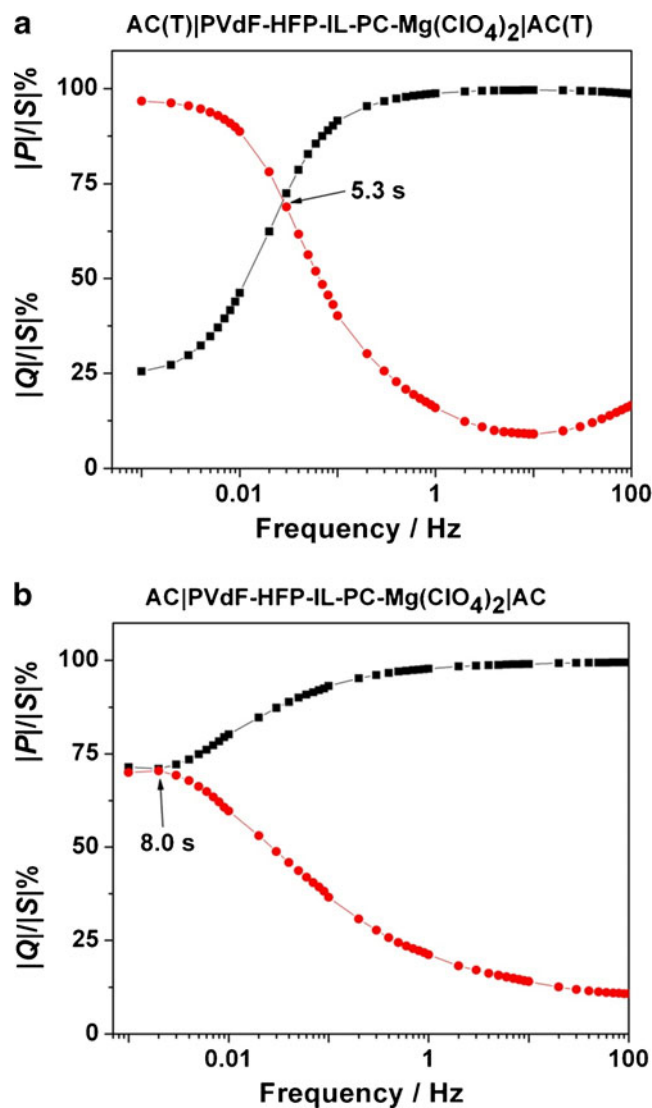


**Fig. 9** Plots of normalized active power  $|P|/|S|$  and reactive power  $|Q|/|S|$  as a function of frequency (in logarithmic scale) for different EDLC cells. **a** Cell A: AC(T) | PVdF-HFP-[EDiMIM][BF<sub>4</sub>]-PC-MgClO<sub>4</sub>)<sub>2</sub> | AC(T). **b** Cell B: AC | PVdF-HFP-[EDiMIM][BF<sub>4</sub>]-PC-MgClO<sub>4</sub>)<sub>2</sub> | AC

It is the microporosity and small particle size of the chemically treated activated charcoal powder that decreases the ion transfer resistance and distances, which gives this material the superior power output ability.

### Cyclic voltammetry

Cyclic voltammetry is an effective tool to reveal the capacitive behavior of the given material. Large current and rectangular forms of the voltammogram, symmetric in anodic and cathodic directions are indications of an ideal capacitive nature [5]. It is carried out either in three-electrode configuration for liquid-based electrolytes or in two-electrode configuration in the case of solid

state-like devices. This technique gives us various kinds of information including nature of charge storage at the individual interfaces in the anodic and cathodic regions and the overall behavior of the capacitor cell. Figure 10a–b shows the cyclic voltammograms (in two-electrode configuration) for the EDLCs (A–B) at different scan rates. In linear sweep cyclic voltammetry technique, the profile is ideally rectangle when capacitance is constant, i.e., it is potential independent. On the other hand, a peak structured voltammogram is observed in the case of potential-dependent capacitance showing a differential profile. In the present study, cyclic voltammogram for both EDLCs (A–B) shows almost featureless characteristics. Also, cyclic voltammetric loops in our experiment are almost rectangle in the case of chemically treated activated charcoal powder electrodes

and nearly rectangle in the case of untreated charcoal powder-based electrodes which confirm the capacitive behavior. It can be seen that capacitive performance of chemically treated activated charcoal-based EDLCs is obviously better than those of untreated charcoal powder-based EDLCs. The featureless characteristics of voltammogram indicates that the electron transfer between the electrodes and gel electrolyte occurs at a constant rate which gives fairly good mirror image of the current responses about the zero current line between the charging and discharging processes of the capacitor cell. The response of each capacitor cell has been found to depend on scan rate, which is the basic characteristic of capacitor cell. The capacitance values of all the cells as calculated using Eq. 2 in the present study have been found to be  $738 \text{ mF cm}^{-2}$  (equivalent to single-electrode-specific capacitance of  $492 \text{ Fg}^{-1}$ ) for EDLC cell A and  $92 \text{ mF cm}^{-2}$  (equivalent to single-electrode-specific capacitance of  $26 \text{ Fg}^{-1}$ ) for EDLC cell B. These values are almost in good agreement with the values obtained from impedance analysis and charge–discharge measurements. This larger value of capacitance for chemically treated-activated charcoal powder is due to its larger surface area as compared to the untreated charcoal powder. The variation of capacitance as a function of scan rate for capacitor cell A has been shown in Fig. 11. Initially, a slight decrease in the values of capacitance has been found at the lower scan rates. Then, almost stable and constant capacitance values have been observed even for a higher scan rate, which indicates the fast ion switching behavior at the interfaces in such gel electrolyte-based EDLCs. This assures the suitability of gel electrolyte for their use in the fabrication of EDLCs/electrochemical supercapacitor.

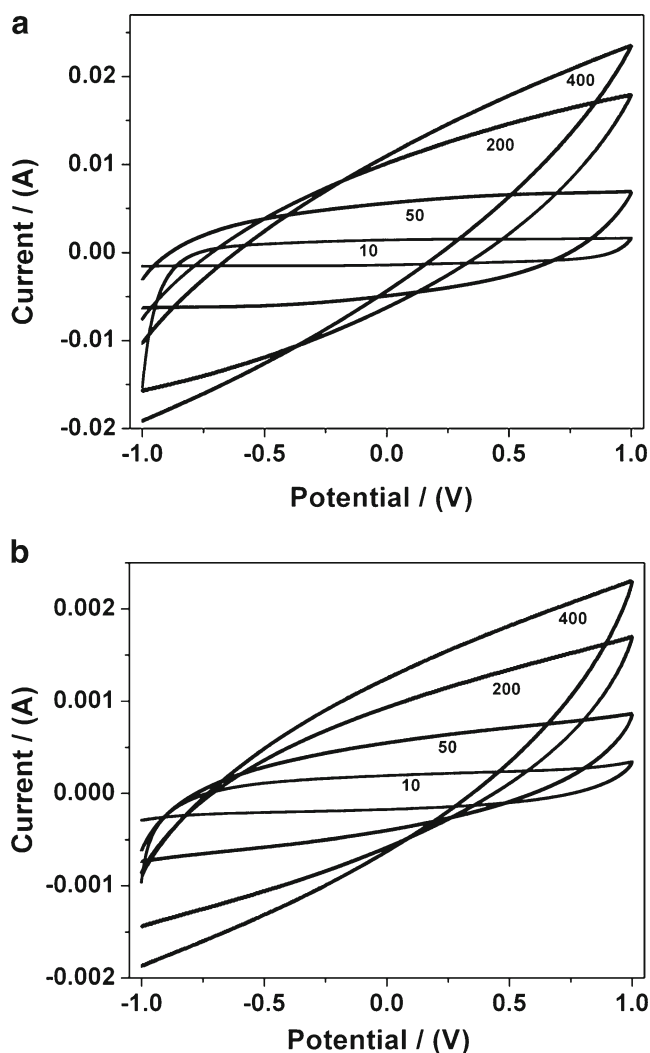


**Fig. 10** Cyclic voltammograms of different EDLC cells at different scan rates. **a** Cell A: AC(T) | PVdF-HFP-[EDiMIM][BF<sub>4</sub>]-PC-MgClO<sub>4</sub>)<sub>2</sub> | AC(T). **b** Cell B: AC | PVdF-HFP-[EDiMIM][BF<sub>4</sub>]-PC-MgClO<sub>4</sub>)<sub>2</sub> | AC

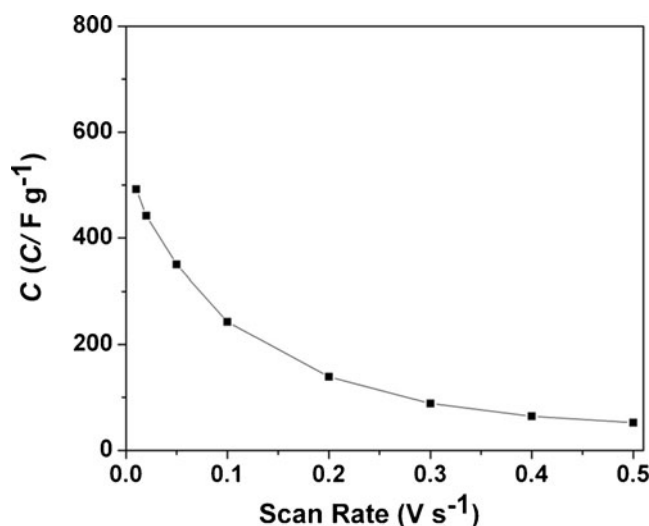


**Fig. 11** Variation of the capacitance of cell A, as a function of scan rates

### Stability and reproducibility

Long cycle life is a crucial and important parameter for EDLC, over rechargeable batteries from the application point of view as an alternative power source to the batteries. The electrochemical stability of chemically treated activated charcoal electrode-based EDLC was evaluated by repeating the cyclic voltammetry test at a scan rate of  $100 \text{ mVs}^{-1}$  for 5,000 cycles. The curves of cell A before charge/discharge test and after 5,000 cycles are shown in Fig. 12 (inset). The specific capacitance of the electrode material as a function of cycle number is presented in Fig. 12. The chemically treated activated charcoal electrode has excellent long cycle life in the entire cycle numbers. It has been observed that almost stable and constant values of capacitance is obtained for cell A up to 5,000 cycles and even more. A slight fluctuation in capacitance values has been observed for initial few cycles, which can be explained by irreversible charge consumption due to some faradic reaction associated with the possible oxidation and reduction of loosely bound surface groups (particularly, hydroxyl group) at the electrode/electrolyte interfaces [5]. After several hundreds of cycles, the interaction force between electrode and electrolyte remain unchanged, implying that the transfer ability of charges would remain fairly constant.

The reproducibility of cell A has also been tested by repetitive recording of cyclic voltammetry (CV). It has been observed that relative standard deviation (RSD) of the specific capacitance for 15 replicate determinations is 3.5 %. Five pieces of chemically treated activated charcoal electrode has been prepared and RSD of individual electrode is found to be 3.6 %. These results clearly indicate that fabricated electrode for EDLC cell A has excellent reproducibility.

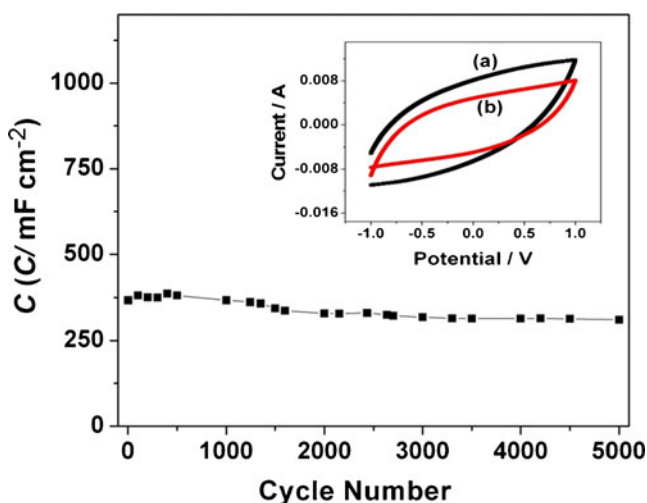


**Fig. 12** Variation of the capacitance of cell A, as a function of voltammetric cycles at a scan rate of  $100 \text{ mVs}^{-1}$ . Inset shows 1st (curve a) and the 5,000th (curve b) cyclic voltammograms of cell A

### Galvanostatic charge–discharge tests

The charge–discharge properties of the EDLCs (A–B) were also investigated by chronopotentiometry and corresponding results are shown in Fig. 13a–b. The cells were charged up to 1.0 V. All the curves exhibit linear and symmetrical images indicating that EDLC cells (A–B) have excellent electrochemical reversibility and capacitive characteristics. The specific capacitance of EDLC cell A at charge–discharge current densities 5, 10, 15, 20, and  $25 \text{ mAcm}^{-2}$  are 396, 345, 327, 302, and  $268 \text{ Fg}^{-1}$ , respectively. The highest specific capacitance of the EDLC cell A ( $396 \text{ Fg}^{-1}$ ) was obtained at  $5 \text{ mAcm}^{-2}$ . When the current density increases to  $25 \text{ mAcm}^{-2}$ , the EDLCs still shows the capacitance value of  $268 \text{ Fg}^{-1}$ . The capacitance retention is nearly 80 %, indicative of a good rate capability. An initial sudden change in the voltage while

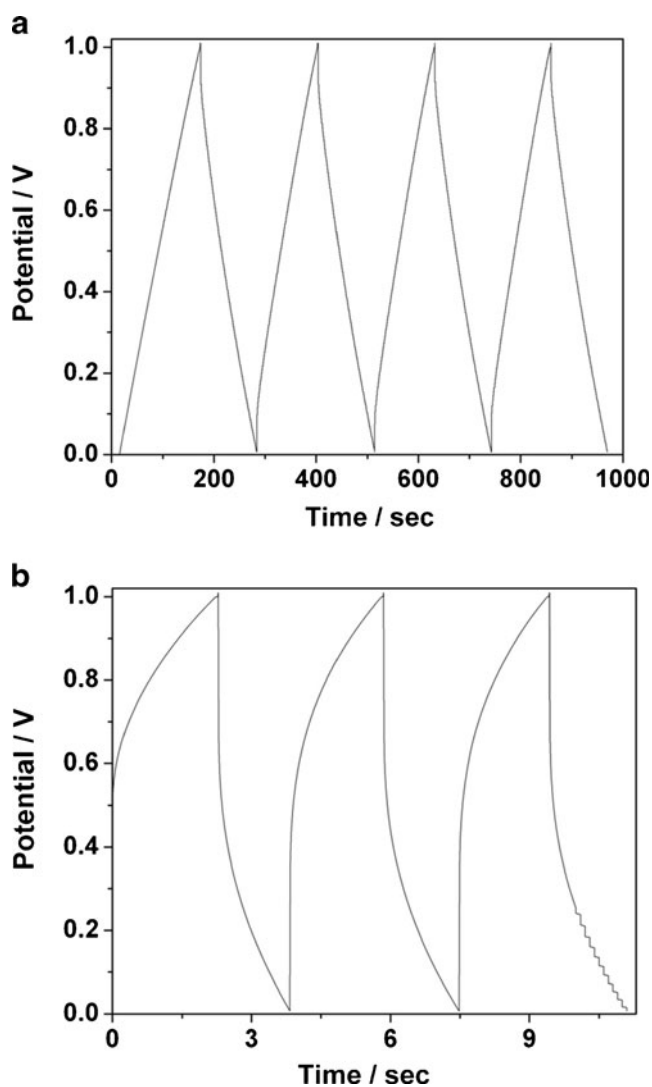


**Fig. 13** Charge–discharge curve of different EDLC cells at a current density of  $5.0 \text{ mAcm}^{-2}$ . **a** Cell A: AC(T) | PVdF-HFP-[EDiMIM][BF<sub>4</sub>]-PC-MgClO<sub>4</sub>)<sub>2</sub> | AC(T). **b** Cell B: AC | PVdF-HFP-[EDiMIM][BF<sub>4</sub>]-PC-MgClO<sub>4</sub>)<sub>2</sub> | AC

**Table 3** Typical charge–discharge characteristics of different EDLC cells at a current density of  $5.0 \text{ mA cm}^{-2}$ 

Cells	$R_i$ ( $\Omega\text{cm}^2$ )	Discharge capacitance, $C_d$		Working voltage (V)	Energy density ( $\text{Whkg}^{-1}$ )	Power density ( $\text{kWkg}^{-1}$ )
		( $\text{mF cm}^{-2}$ ) <sup>a</sup>	( $\text{F g}^{-1}$ ) <sup>b</sup>			
A	10.3	593.7	395.8	1.0	55.0	1.8
B	68.2	15.4	4.4	1.0	0.61	1.3

<sup>a</sup> Overall capacitance of the cells

<sup>b</sup> Single-electrode specific capacitance of the cells

charging and discharging of each cell has been observed, which is due to ohmic loss across internal resistance,  $R_i$ , of the cell. The internal resistances have been calculated from these voltage drops. It may be noted that in the present study, internal resistance values of the chemically activated charcoal powder-based EDLCs are highly reduced as compared to the untreated one. The discharge capacitance,  $C_d$ , values have been calculated from the linear part of the discharge characteristics using Eq. 3. The values of internal resistance,  $R_i$ , and discharge capacitance,  $C_d$ , of EDLC cell (A–B) are listed in Table 3.

The columbic efficiency ( $\eta$ ) was calculated using Eq. 4 and the values to be found in the point of 100 % for an EDLC cell A. Such higher value of columbic efficiency is generally observed for the electrode and liquid electrolyte interfaces. This indirectly suggests the liquidlike ionic conduction behavior of the polymeric gel electrolytes. The energy and power density of a cell (A–B) has also been evaluated and are listed in Table 3.

Figure 14 shows the Ragone plot for cell A. The power densities of fully charged electrodes are plotted as a function of energy density at different current densities varying from 1.0 to  $5.0 \text{ mA cm}^{-2}$ . In this pattern, slowly decreasing

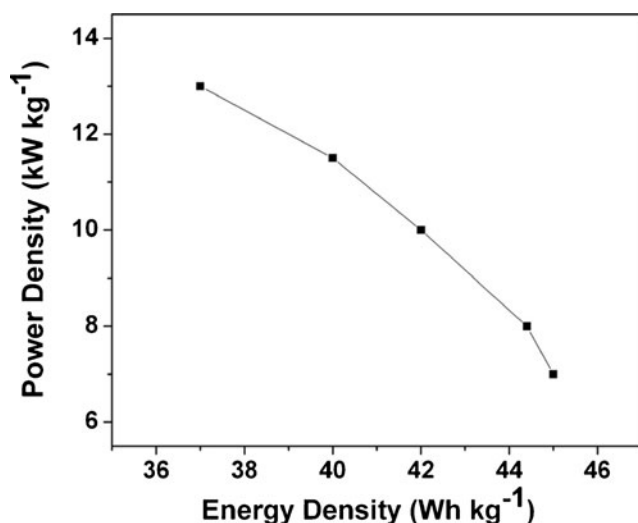


**Fig. 14** Ragone plot related to energy and power densities of cell A with a voltage of 1.0 V

energy density is terminated to a significantly sharper decreasing dependency. The interpretation of the findings basically follows faradic processes, which are slow and encounter a kinetic barrier and the double layer discharge that is fast. The energy and power density values are found in the order of  $55 \text{ Whkg}^{-1}$  and  $2 \text{ kWkg}^{-1}$ , respectively, for cell A and  $0.6 \text{ Whkg}^{-1}$  and  $1.3 \text{ kWkg}^{-1}$  for cell B. It may be noted that energy and power density values are remarkably increased for chemically treated activated charcoal powder-based EDLCs.

#### Influence of porosity on EDLCs

The specific double layer capacitance measured from any of the technique reveals that chemically treated activated charcoal powder-based EDLCs presents the best performance reaching a value of  $579 \text{ F g}^{-1}$ . This value is much higher as compared to one of the best found in the literature for activated carbons with BET surface areas close to  $3,000 \text{ m}^2\text{g}^{-1}$  [55]. It must be noted that the sample with the highest capacitance has BET surface area of only about  $1,500 \text{ m}^2\text{g}^{-1}$  and has almost triple times the capacitance values as obtained from untreated charcoal powder-based EDLCs which has BET surface area of about  $720 \text{ m}^2\text{g}^{-1}$ . This means that some additional factors apart from the surface area are contributing to enhance the capacitance values. It may be explained with an ion sieving effect due to the small pore size of the chemically treated charcoal powder [56, 57]. In case of chemically treated activated charcoal powder, the capacitance goes through a maximum because its porosity is well developed to remove the ion-sieving effect mentioned before. Hence, it is confirmed that porosity is the key parameter for the enhancement of capacitance. As the pores constructed by chemically treated activated charcoal and untreated activated charcoal are mainly micropores with a narrow pore size of  $\sim 3.0 \text{ nm}$  for chemically treated activated charcoal and  $\sim 7.0 \text{ nm}$  for untreated activated charcoal. For faradic pseudocapacitance, the minimum effective pore size should be greater than  $0.8 \text{ nm}$ , while the minimum effective pore size should be greater than  $1.2 \text{ nm}$  for electrochemical double layer capacitance [58]. It should be noted that pore size greater than  $5 \text{ nm}$  is usually loosely bound to the surface layer and do not particularly contribute to the

electrochemical double layer capacitance [59]. Therefore, the pore size in the range of 0.8–5 nm is desirable in order to increase either the pseudocapacitance or electrochemical double layer capacitance. Therefore, in the present study, it is clear that pore size of chemically treated activated charcoal powder is appropriate for increment of electrochemical double layer capacitance. Hence, much higher values of capacitance have been obtained for chemically treated activated charcoal powder over the untreated one.

## Conclusions

From the results presented in the study, it can be concluded that chemically treated activated charcoal powder is successfully prepared in a single stage pyrolysis process. High micropore volume activated carbons (up to  $0.33 \text{ cm}^3 \text{ g}^{-1}$ ) with a quite narrow micropore distribution and BET surface area ( $1,515 \text{ m}^2 \text{ g}^{-1}$ ) have been prepared from a mixture of activated charcoal and KOH by impregnation method. The possibility of the application of chemically treated activated charcoal powder as an electrode material in the fabrication of solidlike EDLCs has been examined. Also, the results have been compared by untreated charcoal powder-based EDLCs. The activated charcoal powder as electrodes with PVdF-HFP–[EDiMIM][BF<sub>4</sub>]-PC-Mg(ClO<sub>4</sub>)<sub>2</sub> as polymeric gel electrolyte have been constructed and characterized using AC impedance analysis, linear sweep cyclic voltammetry, and galvanostatic charge–discharge techniques. Combining all the above results, it may be concluded that:

- The optimized composition of gel polymer electrolyte, PVdF(HFP)–[EDiMIM][BF<sub>4</sub>]-PC-Mg(ClO<sub>4</sub>)<sub>2</sub> shows the room temperature ionic conductivity of  $8.4 \times 10^{-3} \text{ S cm}^{-1}$  in the form of flexible and free-standing films with good dimensional stability, suitable for the fabrication of solidlike EDLCs.
- The present IL-based polymer gel electrolyte appears to be an excellent substitute for the liquid electrolyte in energy storage devices, particularly, in EDLCs.
- In order to achieve maximal value of specific capacitance, chemically treated activated charcoal powder having specific surface area of  $1,515 \text{ m}^2 \text{ g}^{-1}$  with suitable porosity structure has been selected as electrode materials.
- The overall capacitance values have been observed to be  $868 \text{ mF cm}^{-2}$  (equivalent to single-electrode-specific capacitance of  $579 \text{ F g}^{-1}$ ) for chemically treated activated charcoal powder-based EDLCs, whereas it is  $215 \text{ mF cm}^{-2}$  (equivalent to single-electrode-specific capacitance of  $62 \text{ F g}^{-1}$ ) for untreated charcoal powder-based EDLCs.
- The specific energy has been found to be  $55 \text{ Wh kg}^{-1}$  which corresponds to power density of  $2 \text{ kW kg}^{-1}$  for

chemically treated activated charcoal-based EDLCs, whereas it is only  $0.6 \text{ Wh kg}^{-1}$  (energy density) and  $1.3 \text{ kW kg}^{-1}$  (power density) for untreated charcoal powder-based EDLCs.

- The capacitor cell A has reasonably stable capacitance values up to 5,000 voltammetric cycles and even more.
- The comparative study shows that porosity and surface area of electrode plays a vital role in the enhancement of capacitive values. The higher the porosity and surface area of the material, the higher is its capacitive values.
- Columbic efficiency of cell A has been found to be 100 % indicating liquidlike properties of the gel electrolyte.

**Acknowledgments** The authors are grateful to the Department of Science & Technology, Government of India for providing financial support through Grant-in-Aid for Scientific Research (D.O. Nos.: SR/FTP/PS-02/2007; dated 30.07.2008). We are thankful to Dr. S. A. Hashmi, University of Delhi for providing BET results and Prof. A. V. Rao, Shivaji University, Kolhapur for providing SEM results. We extend our sincere thanks to Prof. P.K. Singh, JUET, Guna for many useful discussions and suggestions.

## References

1. Conway BE, Birss V, Wojtowicz J (1997) *J Power Sources* 66:1–14
2. Arico AS, Bruce P, Scrosati B, Tarascon JM, Schalkwijk AV (2005) *Nat Mater* 4:366–377
3. Gupta V, Kusahara T, Toyama H, Gupta S, Miura N (2007) *Electrochem Commun* 9:2315–2319
4. Fan Z, Chen J, Wang M, Cui K, Zhou H, Kuang Y (2006) *Diamond Relat Mater* 15:1478–1483
5. Conway BE (1999) *Electrochemical supercapacitors: scientific fundamentals and technical applications*. Kluwer/Plenum, New York
6. Kotz R, Carlen M (2000) *Electrochim Acta* 45:2483–2498
7. Nishino A (1996) *J Power Sources* 60:137–147
8. Hashmi SA, Upadhyaya HM (2002) *Solid State Ionics* 152:883–889
9. Hashmi SA, Latham RJ, Linford RG, Schlindwein WS (1997) *J Chem Soc Faraday Trans* 93:4177–4182
10. Osaka T, Liu X, Nojima M, Momma T (1999) *J Electrochem Soc* 146:1724–1729
11. Beauharnois ME, Edie DD, Thies MC (2001) *Carbon* 39:2101–2111
12. Lavin JG, Boyington DR, Lahijani J, Nysten B, Issi J-P (1993) *Carbon* 31:1001–1002
13. Pell WG, Conway BE (2004) *J Power Sources* 136:334–345
14. Wang YG, Xia YY (2005) *Electrochem Commun* 7:1138–1142
15. Khomenko V, Raymundo-Piñero E, Beguin F (2006) *J Power Sources* 153:183–190
16. Brousse T, Taberna PL, Crosnier O, Dugas R, Guillemet P, Scudeller Y, Zhou Y, Favier F, Belanger D, Simon P (2007) *J Power Sources* 173:633–641
17. Xue Y, Chen Y, Zhang ML, Yan YD (2008) *Mater Lett* 62:3884–3886
18. Qu Q, Zhang P, Wang B, Chen Y, Tian S, Wu Y, Holze R (2009) *J Phys Chem C* 113:14020–14027

19. Malak A, Fic K, Lota G, Vix-Guterl C, Frackowiak E (2010) *J Solid State Electrochem* 14:811–816
20. Du X, Wang C, Chen M, Jiao Y, Wang J (2009) *J Phys Chem C* 113:2643–2646
21. Qu QT, Shi Y, Li LL, Guo WL, Wu YP, Zhang HP, Guan SY, Holze R (2009) *Electrochem Commun* 11:1325–1328
22. Srinivasan V, Weidner JW (2000) *J Electrochem Soc* 147:880–885
23. Wang J, Xu YL, Chen X, Sun XF (2007) *Compos Sci Technol* 67:2981–2985
24. Wang J, Xu YL, Chen X, Du XF (2007) *J Power Sources* 163:1120–1125
25. Tripathi SK, Kumar A, Hashmi SA (2006) *Solid State Ionics* 177:2979–2985
26. Fan LZ, Maier J (2006) *Electrochem Commun* 8:937–940
27. Sivakkumar SR, Saraswathi R (2004) *J Power Sources* 137:322–328
28. Gomez-Romero P, Chojak M, Cuentas-Gallegos K, Asensio JA, Kulesza PJ, Casan-Pastor N, Lira-Cantu M (2003) *Electrochem Commun* 5:149–153
29. Kulesza PJ, Skunik M, Baranowska B, Miecznikowski K, Chojak M, Karnicka K, Frackowiak E, Beguin F, Kuhn A, Delville MH, Starobrzynska B, Ernst A (2006) *Electrochim Acta* 51:2373–2379
30. Ryu KS, Lee YG, Hong YS, Park YJ, Wu XL, Kim KM, Kang MG, Park NG, Chang SH (2004) *Electrochim Acta* 50:843–847
31. Lewandowski A, Swiderska A (2003) *Solid State Ionics* 161:243–249
32. Zhang YP, Pan LK, Gao Y, Zhang ZJ, Sun Z (2008) *Surf Rev Lett* 15:245–248
33. Hashmi SA, Kumar A, Tripathi SK (2007) *J Phys D Appl Phys* 40:6527–6534
34. Kufian MZ, Majid SR, Arof AK (2007) *Ionics* 13:231–234
35. Hashmi SA, Latham RJ, Linford RG, Schlindwein WS (1998) *Polym Int* 47:2–33
36. Tarascon J-M, Armand M (2001) *Nature* 414:359–367
37. Yoshimoto N, Yakushiji S, Ishikawa M, Morita M (2002) *Solid State Ionics* 152–153:259–266
38. Kumar GG, Munichandraiah N (2002) *Electrochim Acta* 47:1013–1022
39. CS Brazel, RD Rogers (2005) (Eds.) *Ionic liquids in polymer systems*, ACS Symposium Series 913, American Chemical Society, Washington DC
40. Ohno H (ed) (2005) *Electrochemical aspects of ionic liquids*. Wiley, Hoboken
41. Bonhote P, Dias AP, Papageorgiou N, Kalyanasundaram K, Gratzel M (1996) *Inorg Chem* 35:1168–1178
42. Webber A, Blomgrem GE (2002) *Advances in lithium-ion batteries*. In: Scrosati B (ed) Schalkwijk WAV. Kluwer/Plenum, New York, pp 185–232
43. Galinski M, Lewandowski A, Stepniak I (2006) *Electrochim Acta* 51:5567–5580
44. Macfarlane DR, Forsyth M, Howlett PC, Pringle JM, Sun J, Annat G, Neil W, Izgorodina EI (2007) *Acc Chem Res* 40:1165–1173
45. Croce F, Appetechi GB, Mustarelli P, Quartarone E, Tomasi C, Cazzanelli E (1998) *Electrochim Acta* 10–11:1441
46. Grillone AM, Panero S, Retamal BA, Scrosati B (1999) *J Electrochem Soc* 146:27–31
47. Chandra S, Sekhon SS, Arora N (2000) *Ionics* 6:112–118
48. Chandra S, Sekhon SS, Srivastava R, Arora N (2002) *Solid State Ionics* 154:609–619
49. Keiser H, Beccu KD, Gutjahr MA (1976) *Electrochim Acta* 21:539–543
50. Wang J, Chen M, Wang C, Wang J, Zheng J (2011) *J Power Sources* 196:550–558
51. Cole KS, Cole RH (1941) *J Chem Phys* 9:341
52. Miller J (1998) in *Proceedings of the 8th International Seminar on Double-Layer Capacitors and Similar Energy Storage Devices*, Deerfield Beach, FL Dec 7–9
53. Lust E, Janes A, Arulepp M (2004) *J Electroanal Chem* 562:33–42
54. Taberna PL, Simon P, Fauvarque JF (2003) *J Electrochem Soc* 150:A292–A300
55. Keirzek K, Frackowiak E, Lota G, Gryglewicz G, Machnikowski J (2004) *J Electrochim Acta* 49:515–523
56. Lozano-Castello D, Cazorla-Amoros D, Linares Solano A, Shiraishi S, Kurihara H, Oya A (2000) *Carbon* 41:1765–1775
57. Gryglewicz G, Machnikowski J, Lorenc-Grabowska E, Lota G, Frackowiak E (2005) *Electrochim Acta* 50:1197–1206
58. Cao L, Lu M, Li H-L (2005) *J Electrochem Soc* 152:A871–A875
59. An K, Kim W, Park Y, Choi Y, Lee S, Chung D, Bae D, Lim S, Lee Y (2001) *Adv Mater* 13:497–500